Desalination 574 (2024) 117179

Contents lists available at ScienceDirect

Desalination

journal homepage: www.elsevier.com/locate/desal

Coion exclusion properties of cation exchange membranes in 2:1 divalent salt solutions

Zheng Jie Lim [a,1], Marcus Kho [a,1], William Toh [b], Xiao Chen [c,*], K.B. Goh [a,*]

[a] Department of Mechanical Engineering, School of Engineering, Monash University Malaysia, Jalan Lagoon Selatan, 47500 Bandar Sunway, Selangor, Malaysia
[b] School of Mechanical and Aerospace Engineering, Nanyang Technological University, 50 Nanyang Avenue, Singapore 639798, Singapore
[c] Institute of Biomechanics and Medical Engineering, Department of Engineering Mechanics, Tsinghua University, Beijing 100084, China

HIGHLIGHTS

- A molecular theory is proposed to capture coion exclusion property of IEM.
- Coions exist in condensed state when IEM operates in low-salt concentrations.
- Coions exist in free state when IEM operates in high-salt concentrations.
- Our theory works across different concentrations of 2:1 salt solutions.

GRAPHICAL ABSTRACT

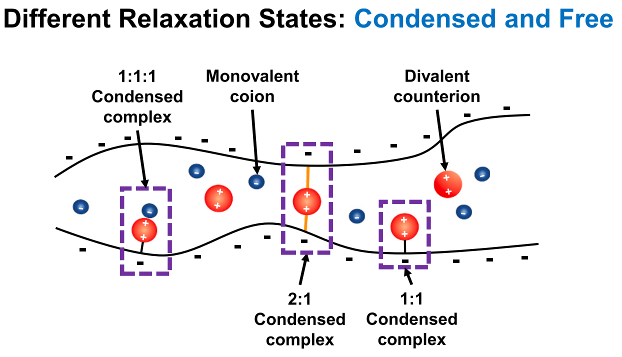

ARTICLE INFO

Keywords:
Coion
IEMs
Condensation
Theoretical model
Donnan potential

ABSTRACT

The selectivity of ion exchange membranes hinges on their capacity to exclude coions. Yet, understanding how they reject coions in multivalent salt solutions remains challenging. This study presents a new molecular theory to understand coion exclusion. It examines counterion and coion condensation, including electrosteric effects. Supported by experimental data [Gokturk et al., Nat. Commun., 13 (2022)], we analyze cation exchange membrane potential in a 2:1 salt solution, revealing insights into coion selectivity and exclusion mechanisms. Notably, our theory deviates from earlier research by accommodating condensed divalent counterions that bind to one or two fixed-charged monomers. Additionally, we account for many-body electrostatic interactions, allowing the former to bind to sorbed coions. Our findings highlight the importance of coion condensation, especially in low-concentration salt conditions where coions are mainly condensed. This effect becomes less significant as the external solution concentration rises. These findings clarify the suitability of the ideal Donnan model in high-concentration salts, but its accuracy decreases in low-concentration situations. To summarize, our study emphasizes the need to account for counterion and coion condensation to understand membrane selectivity in low-concentration multivalent salt solutions.

---

* Corresponding authors.
E-mail addresses: chenxiao2021@tsinghua.org.cn (X. Chen), kekboon.goh@monash.edu (K.B. Goh).

[1] These authors contributed equally to this work.

https://doi.org/10.1016/j.desal.2023.117179
Received 29 August 2023; Received in revised form 27 October 2023; Accepted 18 November 2023

1. Introduction

Ion exchange membranes have garnered significant attention for their selective ion transport capabilities, rendering them indispensable for various membrane-based technologies, such as electrodialysis, fuel cells, and catalytic reactors [1–5]. Typically, these membranes comprise crosslinked polymeric chains functionalized with a univalent anionic/cationic fixed charge group, creating a charged microenvironment. When immersed in salt solutions, these charged ion exchange membranes sorb counterions and exclude coions, modulated by the fixed charged group [6,7]. However, there has been limited systematic fundamental research into coion transport through polymeric membranes immersed in multivalent salt solutions [8–11]. As a result, this has left the coion exclusion behavior incompletely understood, as it deviates from the (standard) idealized Donnan description, especially in low-concentration salt regime [8,12–17]. In principle, when coions transport through charged membranes, e.g., ion exchange (IE), reverse osmosis (RO), and nanofiltration (NF), they can condense onto the crosslinked polymeric chains, via a previously formed complex, involving multivalent counterions and univalent charged monomers (on the fixed group) [13,18–21]. Researchers often overlook the phenomenon of site-bound coion condensation when describing the selectivity performance of these membranes. Considering conventional practices, we examine the impact of coion condensation on the selectivity of cation exchange membranes operating in 2:1 salt solutions in this work.

While coion exclusion plays a pivotal role in unraveling the performance of ion exchange membranes, its underlying mechanism remains incompletely understood [22]. When we equilibrate these membranes in salt solutions, an electrical potential develops at the membrane-solution interface, a phenomenon termed the Donnan potential, arising from ionic imbalances. This potential governs the exclusion of coions, contributing to membrane selectivity based on electrical charge. However, in the realm of theoretical chemical and polymer physics, multiple studies underscore the significance of accounting for the many-body nature of electrostatic interactions involving coions and the complex formed by multivalent counterions and fixed charged monomers, a phenomenon referred to as coion condensation [19,20,23,24]. Within this context, Muthukumar's research group introduced a molecular-level framework that illustrates how coions condense to charged polymeric chains within a polyelectrolyte solution [20,24]: they used the interaction between a univalent fixed charge group on the polymeric chains and a multivalent/divalent counterion. For simplicity, let us term this interaction a “1:1” relationship (representing one fixed charged monomer to one multivalent counterion), distinct from the “1:1/2:1” salt solutions. This 1:1 interaction creates a complex with a local net charge. Subsequently, the many-body nature of electrostatic forces allows the condensation of a coion to this 1:1 entity to neutralize the local charge, forming a newer “1:1:1” complex composed of one fixed charged monomer, one multivalent counterion, and one coion [20,24]. To summarize, the presence of condensed multivalent counterions indirectly promotes the physical binding/condensation of coions to the charged polymeric chains. To this end, we hypothesize that this phenomenon may, in turn, have a regulatory effect on the coion exclusion property of the membranes.

The comprehensive understanding of different sorbed coion relaxation states in a molecular context, mainly free/mobile and condensed/paired, remains an ongoing theoretical endeavor. The limitations of the conventional ideal Donnan model's depiction of coion and counterion permeation through charged membranes become especially apparent when considering its applicability to scenarios involving salt solutions containing multivalent ions [25]. In other words, this standard, ideal model overlooks the presence and significance of the condensed counterions and coions in modulating the membranes' transport properties. While the Donnan theory effectively accounts for coion exclusion into hydrated ion exchange membranes immersed in high-concentration 2:1 salt solutions (e.g., calcium chloride), its applicability falters in low-concentration salt solutions or when dealing with dehydrated membranes [8,13,25,26]. In such scenarios, the mechanics of coion exclusion by these membranes may vary when operating in low-salt and high-salt solution regimes. Additionally, the propensity for ions, coions, and counterions to condense to the polymeric chains in these membranes is notably higher in divalent salt solutions compared to their monovalent counterparts [25,27,28]. To this end, the heightened condensation effect further departs the ion partitioning from the idealized Donnan picture. To address these complexities, Freeman's research group integrated Manning's theory of counterion condensation (territorial condensation) with the Donnan theory [29,30]. Furthermore, our recent works underscore a recent endeavor to capture the impact of counterion ion-pairing (site-bound condensation) within such membranes [13,25]. Although our investigations have yielded progress in comprehending counterion partitioning, we acknowledge encountering hurdles in precisely characterizing the partitioning behavior of coions [13]. Notably absent from these approaches is the consideration of coion condensation, particularly of the site-bound variety, and its role in modulating the transport properties of charged membranes operating in multivalent salt environments.

Here, we tackle a crucial inquiry: the influence of coion condensation on the selectivity performance of ion exchange membranes. To examine this problem, we present a molecular theory that explicitly considers site-bound (a) coion and (b) counterion condensations. This theory enables us to quantify coion partitioning, at the molecular level, in ion exchange membranes when immersed in 2:1 salt solutions (e.g., magnesium/calcium chloride). For completeness, we account for four general sorbed counterion and coion states in the ion exchange membranes; namely, (i) condensed divalent counterion with no coion, (ii) condensed divalent counterion with monovalent coion, (iii) free divalent counterion, and (iv) free monovalent coion (see Fig. 1). Specifically, we allow the condensed counterion to exist in either (I) a bridged (two fixed charged monomers to one divalent counterion binding, 2:1 interaction) [31] or (II) a non-bridged (one fixed charged monomer to one divalent counterion binding, 1:1 interaction) state, as illustrated in Fig. 1. Additionally, we explore the formation of a new complex involving the latter configuration (II) along with free coions, creating a complex involving one fixed charged monomer, one divalent counterion, and one coion (1:1:1 interaction). To establish a tight connection between our theoretical framework presented here to real-life membranes, the theory also considers the ion–water–membrane interactions: intra and intermolecular effects (via a packing constraint), and (electrostatic and dielectric) electrical factors, in addition to the counterion- and coion-condensation interactions. To validate our theoretical results, we compare them with published experimental data, demonstrating the validity of our theory. Through this approach, we quantify the distribution of different coion relaxation states within the membranes, shedding light on the impact of coion condensation on the transport properties of the membranes. In essence, our method allows us to elucidate the local partitioning of coions between the polymeric chains within the membranes and their surrounding interstitial solutions, enabling us to assess the significance of condensed coions in governing partitioning across such membranes.

2. Methodology

2.1. Problem statement: how sorbed counterions and coions relax in cation exchange membranes

This section attempts to understand how divalent counterions and monovalent coions mutually equilibrate in a cation exchange membrane when operating in a divalent 2:1 salt solution, as illustrated in Fig. 1. The membrane, in principle, contains different sorbed free and condensed ions and fixed, charged monomers. For completeness, we take into account water molecules in our theoretical formulation through a molecular incompressibility expression (see Eq. (7)), allowing us to reduce our parameter space [32]. Here the framework proposed by Muthukumar's works is employed [20,24], in which, as visualized in Fig. 1, the fixed charge group on the monomer can exist in the following states: (i) one monomer to one divalent counterion to one monovalent coion (we term 1:1:1 interaction, i.e., condensed counterion-coion, c_C^P), (ii) two monomers to one divalent counterion (we term 2:1 interaction, i.e., ion bridge formed by condensed counterion, c_B^P) and (iii) one monomer to one divalent counterion (we term 1:1 interaction, i.e., condensed counterion without coion, $c_{B'}^P - c_C^P$). For completeness, we also allow the sorbed (iv) divalent counterions and (v) monovalent coions to be in diffusive/free states [33]. For consistency, the notation established in Muthukumar's previous works is also adhered to [20,24]. Henceforth, "site-bound condensation" and "physical binding" terms are used interchangeably for simplicity.

For consistency, the assumptions specified in our previous works are also adhered to [13,25]. These assumptions comprise the following: (a) Dominance of site-bound/ion pairing-type condensation effects in the interaction between fixed charged monomers and sorbed multivalent counterions. (b) The membrane upholds an electroneutrality condition. (c) Unlike our earlier studies, the constraint of negligible coion condensation is no longer imposed. (d) The scenario in which a divalent counterion binds to two adjacent charged monomers along the same polymer chain is disregarded. The omission originated from the assumption that the charged monomers are sparsely distributed along the chain. Consequently, the probability of forming ion bridges between two separate polymer chains is significantly higher than the likelihood of a divalent ion binding to two adjacent monomers within a single chain.

2.2. *Free energy functional formulation*

In this subsection, we aim to present the membrane's free energy functional employed in our framework, denoted as W, under the influence of a 2:1 divalent salt solution. By utilizing this functional, W, we can comprehensively account for the membrane's electrical, physical, and chemical characteristics. This free energy functional, W, accounts for the different condensation states for sorbed counterions and coions, as well as the behavior of sorbed mobile/free ions within the systems. To achieve this objective, we first introduce the concept of condensation-free energy, labeled as F_{cond}, which finds the mathematical definition in Eq. (1). We guide interested readers to the Supplementary Information (SI) section for a detailed derivation.

$$\begin{aligned} F_{cond} = & \int \{ (\rho_{B'}^P - \rho_C^P) \Delta U_1 + \rho_C^P \Delta U_2 + \rho_B^P \Delta U_3 \} \mathrm{d}\boldsymbol{r} \\ & + \frac{1}{\beta} \int \Big\{ - \rho_F ln N_F + (\rho_F - \rho_{B'}^P - 2\rho_B^P) ln(N_F - N_{B'} - 2N_B) \\ & + (\rho_{B'}^P - \rho_C^P) ln(N_{B'} - N_C) + \rho_C^P ln N_C + 2\rho_B^P ln N_B + \rho_B^P ln 2 \} \, \mathrm{d}\boldsymbol{r} \end{aligned} \tag{1}$$

where $\rho_F, \rho_B^P, \rho_{B'}^P, \rho_C^P$ are the number concentration, i.e. particle number per swollen volume ($\#/\mathrm{m}^3$) of fixed charge group, bridged divalent counterions (2:1 two monomer–one divalent counterion interaction), non-bridged condensed counterions (a) 1:1 one monomer–one divalent counterion and b) 1:1:1 one monomer–one divalent counterion–one coion interactions), and condensed monovalent coions, respectively. N_F, $N_B^P, N_{B'}^P, N_C^P$ are the number of fixed charge group, bridged divalent counterions, non-bridged condensed counterions and condensed

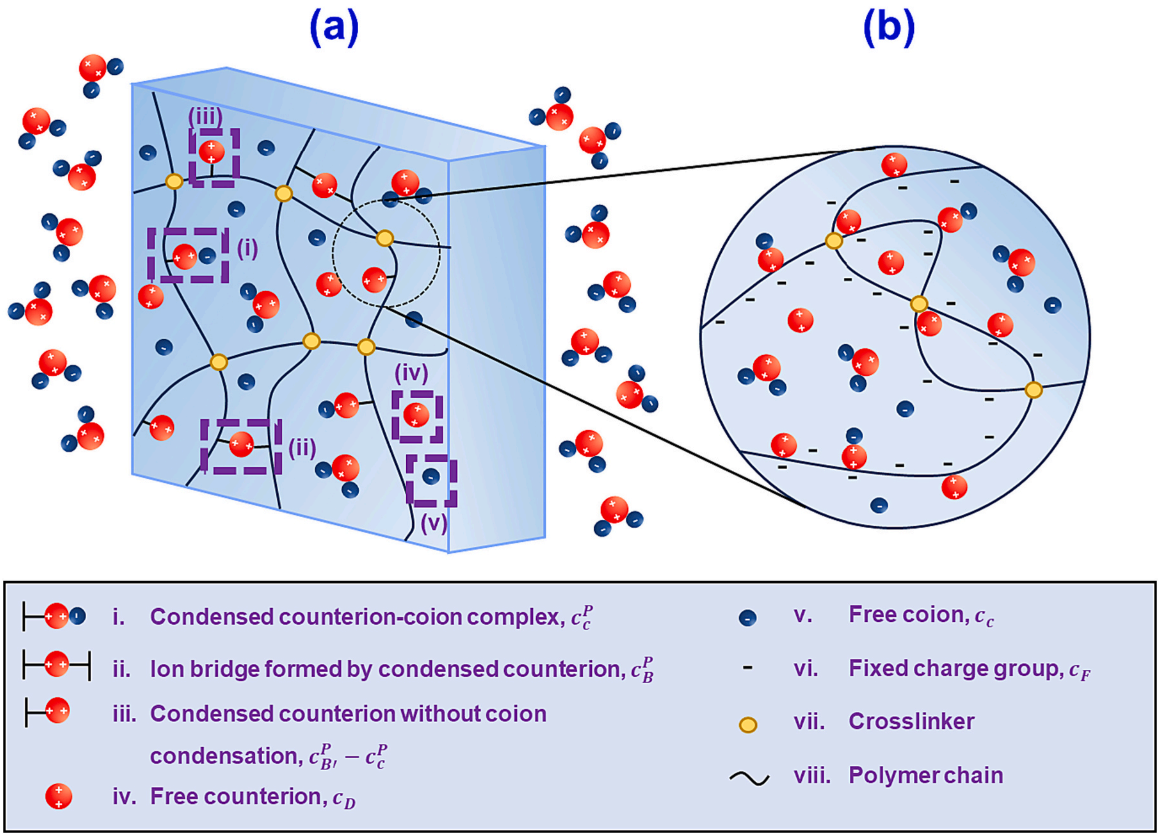

Fig. 1. (a) Schematic illustration of a cation exchange membrane immersed in a 2:1 salt solution consisting of divalent counterions and monovalent coions and (b) its microscopic view. Here we adopt a few different condensation states with each charged monomer: (i) one monomer to one divalent counterion to one monovalent coion (termed 1:1:1 interaction, i.e., condensed counterion-coion, c_C^P), (ii) two monomers to one divalent counterion (termed 2:1 interaction, i.e., ion bridge formed by condensed counterion, c_B^P) and (iii) one monomer to one divalent counterion (termed 1:1 interaction, i.e., condensed counterion without coion, $c_{B'}^P - c_C^P$). For completeness, we also allow the sorbed (iv) divalent counterions and (v) monovalent coions to be in diffusive/free states.

monovalent coions, $\boldsymbol{r}$ represents the position vector and ΔU is the ion binding energy. The term β is defined as $\beta = 1/k_BT$, where k_B is the Boltzmann constant and T is the temperature.

In the context of the (a) direct (monomer–divalent counterion complexation) and (b) indirect (coion and monomer–divalent counterion complexation) condensations to the monomers on the polymeric chains, the free energy functional, W, in general, arises from a combination of enthalpic and entropic influences—the first term on the right hand side of Eq. (1) captures the enthalpic contribution, which originates from the temporary, physical binding/site-bound condensation between the monomers and the sorbed ions. In more comprehensive terms, forming physical bindings or site-bound condensation between the monomer and ions leads to a more substantial enthalpic contribution, negatively affecting the condensation-free energy, F_{cond}. Conversely, the entropic part is more convoluted to capture mathematically. The formation of the physical binding reduces the translational entropy of the ions. During condensation, the monomers and counterions adopt distinct molecular configurations, leading to fewer possible molecular arrangements than their free states before condensation. As a result, these phenomena impose an entropic cost into the functional captured by the second term on the right hand side of Eq. (1) [21,34]. In summary, we elucidate the two–stage coion condensation process by examining the interplay between entropy and enthalpy contributions when the sorbed counterions and coions condense, directly or indirectly, with the fixed charged monomers in the membranes, as explained above.

The Helmholtz free energy F of our membrane, as formulated in our previous work, is expressed as follows [13,25]

$$F = F_{idea} + F_{elec} + F_{Born} + F_{cond} \tag{2}$$

Here, we will break down the Helmholtz free energy F into four terms. The first term will correspond to the ideal energy, which will account for the translational entropy of all diffusive species, including counterions, coions, and water molecules. The second term will characterize the electrostatic energy as dictated by the density/concentration of the charged species in the membranes, encompassing both the mobile ones (diffusive ions) and the immobile ones (fixed charge and condensed groups). The third term will represent the Born energy, quantifying the change in free energy when transferring an ion across two dielectric media, namely, the external solution and the membrane [35]. Finally, the last term will describe the contribution of ion condensation between the ions and the monomer of the fixed charge group.

The first three terms are explicitly given here [13,25,36]

$$F_{idea} = \frac{1}{\beta}\int\left\{\rho_w(ln\rho_w v_w - 1) + \sum_i \rho_i(ln\rho_i v_w - 1)\right\}d\boldsymbol{r} \tag{3}$$

$$F_{elec} = \int\left\{\left(z_F\rho_F + \sum_i z_i\rho_i + \sum_j z_j\rho_j^P\right)e\Psi - \frac{1}{2}\epsilon\epsilon_0(\nabla\Psi)^2\right\}d\boldsymbol{r} \tag{4}$$

$$F_{Born} = \int\left\{\sum_i \frac{\rho_i z_i^2 e^2}{8\pi\epsilon\epsilon_0 a_i}\right\}d\boldsymbol{r} \tag{5}$$

where ρ_w, ρ_F, ρ_i, and ρ_j^P represent the number concentration, per swollen membrane volume, of water molecules, monovalent fixed charge group, mobile ion i, and condensed ion j ($i = \text{D, C}$ and $\text{j} = \text{B, B}', \text{C}$, where divalent counterion is "D", monovalent coion is denoted as "C", bridged counterion is referred as "B" and non-bridged counterion is "B′"), respectively. The characteristic volume of a water molecule is represented by v_w. The valencies of the mobile ion (i), condensed ion (j), and monovalent fixed charge group are denoted by z_i, z_j, and z_F, respectively. Additionally, key electric properties are denoted as follows: the electric potential is represented by Ψ, the hydrated radius of ion i is given by a_i, the elementary unit of charge is symbolized as e, the vacuum permittivity is marked as ϵ_0, and the relative permittivity of the membrane material is denoted as ϵ.

Swollen ion exchange membranes are primarily composed of cross-linked polymeric chains immersed in an interstitial solution, predominantly consisting of water. As a result, the relative permittivity of these membranes is notably influenced by the combined effects of these constituents. The equation depicting the relative permittivity of the membrane can be represented as follows [13,35,37]

$$\epsilon \approx \epsilon_P\phi_P + \epsilon_w\phi_w \tag{6}$$

where ϵ_P and ϵ_W stand for the relative permittivities of the polymer and water, respectively, while ϕ_P and ϕ_w denote the corresponding polymer and water volume fractions with respect to the volume of the membrane, V. Specifically, the volume fraction ϕ is defined as $\int\rho v\, d\boldsymbol{r}/V$.

We introduce a pair of constraints to complete our free energy functional formulation, denoted as W. These constraints enforce the notions of volume packing and global electroneutrality within our framework. We postulate that the presence of water and polymer molecules, alongside ions, effectively occupies the entirety of the membrane's accessible space. This collective occupancy establishes the membrane's incompressibility condition, as elucidated below [13]

$$\phi_w + \phi_P + \sum_i \phi_i + \sum_j \phi_j^P = 1 \tag{7}$$

In short, Eq. (7) enforces the conservation of mass into our framework by summing the volume fractions of water, ϕ_w, polymer, ϕ_P, mobile ions, ϕ_i, and condensed ions, ϕ_j^P, to unity.

Furthermore, global electroneutrality constraint is also considered, given by [13]

$$\int\langle\rho(\boldsymbol{r})\rangle d\boldsymbol{r} = 0 \tag{8}$$

where $\langle\rho(\boldsymbol{r})\rangle$ is the local mean charge density at location $\boldsymbol{r}$.

Collectively, our semi-grand canonical free energy functional, W, can be presented as follows

$$\begin{aligned} W = \ & F + \int\Pi(\boldsymbol{r})\left(\phi_w + \phi_P + \sum_i \phi_i + \sum_j \phi_j^P - 1\right)d\boldsymbol{r} + \int\lambda\langle\rho(\mathbf{r})\rangle d\mathbf{r} \\ & - \int\rho_i\mu_i d\boldsymbol{r} - \int\rho_w\mu_w\, d\boldsymbol{r} \end{aligned} \tag{9}$$

We introduce two Lagrangian multipliers Π and λ to incorporate the volume packing and electroneutrality constraints into the free energy functional, W. Notably, Π is the position-dependent osmotic pressure that enforces the packing constraint locally, and λ is a reference for the electrical potential. Lastly, μ_D, μ_C and μ_w represent the chemical potential of mobile divalent counterions, mobile monovalent coions and water respectively [13].

2.3. *Minimization of free energy functional*

To obtain the partition ratio of the sorbed mobile ions, ρ_i, we can minimize the free energy functional, W, by solving the equation $\delta W[\rho_i]/\delta\rho_i = 0$, resulting in the following expression (refer to Supplementary Information for detailed steps of the minimization process):

$$\frac{\rho_i}{\bar{\rho}_i} = exp\left[\beta\left\{(\bar{\Pi} - \Pi)v_i + z_i e(\bar{\Psi} - \Psi) + \frac{z_i^2 e^2}{8\pi\epsilon_0 a_i}\left(\frac{1}{\bar{\epsilon}} - \frac{1}{\epsilon}\right)\right\}\right] \tag{10}$$

We note that the variables in the external salt solution are indicated with an overbar symbol.

Additionally, minimization of the free energy functional, W, with respect to nominal concentration of paired ions, ρ_j^P yields the following few expressions, namely

$$\frac{\rho_C^P}{\rho_{B'}^P - \rho_C^P} = exp\left[\beta\left(\Delta U_1 - \Delta U_2 + e\varPsi - \Pi v_C^P\right)\right] \tag{11}$$

$$\frac{\rho_{B'}^P - \rho_C^P}{\rho_F - \rho_{B'}^P - 2\rho_B^P} = exp\left[\beta\left(-\Delta U_1 - 2e\Psi - \Pi v_{B'}^P\right)\right] \tag{12}$$

$$\frac{\rho_B^P}{\rho_F - \rho_{B'}^P - 2\rho_B^P} = \frac{1}{\sqrt{2}}exp\left[\frac{\beta}{2}\left(-\Delta U_3 - 2e\Psi - \Pi v_B^P\right)\right] \tag{13}$$

We can write the total condensed counterion density (molar concentration), mathematically, as $c_D^P = c_B^P + c_{B'}^P$. It is noted the molar concentration, c, can be converted to number concentration, ρ, via this relationship: $\rho = cN_A$, where N_A is the Avogadro constant.

When we minimize the functional, W, with respect to electric potential, Ψ, we obtain our Poisson expression [13,34]

$$\nabla(\epsilon\epsilon_0\nabla\Psi) = \left[\rho_F + \rho_C^P - 2\rho_B^P - 2\rho_{B'}^P - 2\rho_D + \rho_C\right]e \tag{14}$$

Lastly, minimizing the functional W with respect to the number concentration of water, ρ_w, yields the osmotic pressure difference between the interstitial solution and the external solution. This is given by the following expression:

$$\bar{\Pi} - \Pi = \frac{1}{\beta v_w} ln\frac{\phi_w}{\bar{\phi}_w} \tag{15}$$

This theoretical framework offers a self-consistent approach to quantifying condensed monovalent coions and divalent counterions within these charged membranes. These counterions have the ability to physically bind with either one or two charged monomers. To the best of our knowledge, this stands in stark contrast to existing works within the field of membrane science.

In principle, the model can also be employed for anion exchange membranes, assuming the salt solution conforms to a 1:2 type, such as sodium carbonate (Na_2CO_3). Moreover, this also necessitates altering the valency of the fixed charge group to a positive one, namely $z_F = +1$. Typically, the polymer volume fraction in ion exchange membranes increases when their surrounding temperature increase exceeds a certain critical volume transition point. Nevertheless, we contend that, given our ion exchange membranes' exposure to a salt concentration that induces dehydration compared to virgin membranes (i.e., they are dense systems), any temperature-induced volume transition in the system will not introduce new physics. Instead, it will merely scale the equilibrium ion transport property, up and down, offering no substantial new insights. As part of our future work, we plan to test this hypothesis to assess the impact of temperature variations on ion transport properties.

To close, we now list the limitations of our work here. Currently, our model lacks the capability to directly consider (i) the specific interactions between mobile ions and (ii) the variation in salt concentration-dependent water volume fractions of ion exchange membranes, factors that are prominent in solution-membrane systems with salt concentrations exceeding 1 mol/L. Furthermore, our model also lacks the capability to account for the temperature-responsive membrane volume fraction. Incorporating the alteration in polymer volume fraction in response to environmental temperature necessitates a new physics added into the current framework, such as the Flory-Rehner framework, which exceeds the scope of our current study.

3. Validation: connecting our theory to real membrane

We demonstrate the capability of our theory by conducting a comparative analysis between our numerical results and the experimental data presented by Freeman and Crumlin in their study on ion exchange membranes exposed to a 2:1 salt solution, specifically using magnesium chloride ($MgCl_2$) [38]. We depict this relationship in Fig. 2, where our findings exhibit good agreement with the reported experimental data. In particular, our investigation centers around the electrical potential, Ψ, of the ion exchange membrane (Donnan potential), as influenced by the 2:1 salt solution. Based on our current understanding, the potential, Ψ, plays a pivotal role in determining the performance of coion exclusion [39]. Consequently, we are examining our theory's capability to capture and explain this phenomenon accurately. The fixed charge group density, derived from the ion exchange capacity of the membrane and essential to our analysis, is determined to be 3.0 (mol charged groups)/L (sorbed water), following the published parameters [38]. Consistent with our previous work, we estimated values for the volume (v_j^P) and the intrinsic binding energy ($\Delta U_{1/2/3}$) to capture the experimental results. In the Supplementary Information (SI), our readers can locate a comprehensive breakdown of the simulation input parameters.

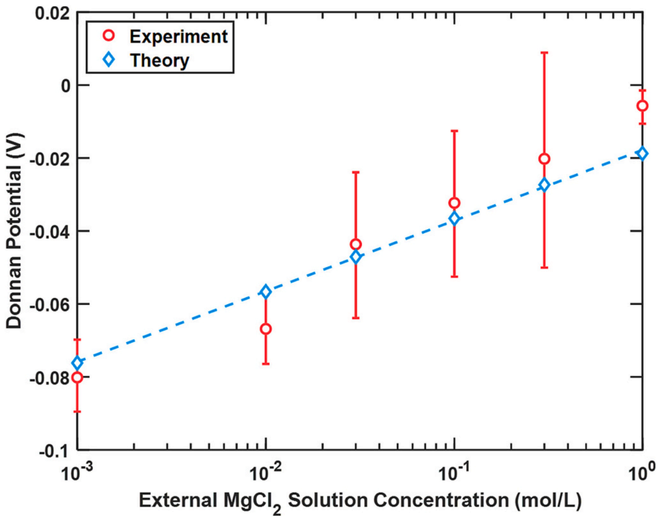

Fig. 2. Electrical potential, Ψ, of cation exchange membrane as a function of external 2:1 salt solution concentration: theory (blue) versus published experimental data (red) [38].

Fig. 2 shows that the strength of the electrical potential, Ψ, decreases with the increase of the external 2:1 salt solution concentration. In the low-concentration external salt solution regime, the more significant ionic imbalance between the membrane and the external solution gives rise to a higher electrical potential, Ψ, intensity. To this end, the external coions require higher energy to overcome the energy barrier at the interface (see Eq. (10)). That is, we expect the sorbed coion concentration to be smaller compared to its counterion counterpart in the membrane. As the external salt concentration enlarges, we expect the sorbed coion and counterion concentrations to increase significantly, balancing the ionic inequality between the membrane-external solution interface, thereby decreasing the electrical potential, Ψ. Compared to a 1:1 external salt solution system, both demonstrate a linear decreasing strength of the electrical potential, $\varPsi$, with the increase of external salt concentration [32,38]. However, we expect the membrane–2:1 external salt solution system to register a lower potential value, at the same external solution concentration, due to the double charges on the sorbed counterions.

To facilitate a comprehensive comparison between our numerical simulations and the experimental measurements, we delve into the results in further detail. Taking into account the variability represented by error bars in the experimental measurements, we find that our numerical results align notably well with the experimental results. However, a distinct, yet minuscule, discrepancy emerges at a higher salt concentration of 1 mol/L, which prompts a deeper exploration of its implications. Water uptake experiments reveal membranes exposed to higher-concentration solutions tend to dehydrate [8], yet our simulation assumes a consistent water volume fraction, ϕ_w, across concentrations. This experimental measurement implies that by decreasing the water volume fraction, ϕ_w, the ionic concentration effectively increases, predicting a reduction in ionic imbalance between the membrane and external solution, consequently lowering electrical potential intensity Ψ, as seen in the measurement results in Fig. 2. Fortunately, our assumption holds, as our numerical results differ from published data by less than 10 %, globally, justifying the constant water volume fraction, ϕ_w, of 0.5 assumption.

For clarity, we primarily focus on assessing the global error, E, rather than individual discrepancies, using the following formula [40]:

$$E = \frac{1}{|u_k|_{max}} \sqrt{\frac{1}{N}\sum_{k=1}(u_k - u_k^r)^2} \tag{16}$$

where E is defined as the global error for our solution, N represents the number of experimental data points, u_k denotes the experimental data at the k-th data point, and u_k^r represents the numerical result at the k-th data point.

4. Results and discussion

In this section, we delve into the distribution of ions between the interstitial solution and the polymeric chains, examining the behavior of sorbed coions and counterions. By analyzing the locally charged environment in the membranes, we enhance the existing dataset reported by Freeman and Crumlin [38]. Through this analysis, we reveal previously inaccessible essential experimental variables, particularly quantifying the (free/mobile and condensed/paired) relaxation states of the sorbed ions. Herein, we use the terms (i) “paired” and “site condensed” and (ii) “mobile” and “free” interchangeably. Unlike other studies in the field of membrane science, we enable the sorbed coion to form a (ionic) physical bond with the charged monomer–divalent counterion complex, allowing us to assess the partitioning of the coion between two distinct environments: (a) the interstitial solution and the polymeric chains, and (b) the membrane and the external divalent 2:1 salt solution. Offering an additional interpretation of the experimental measurements through our theoretical results improves our understanding of the behavior of the sorbed ions and provides valuable insights for assessing the selectivity performance of the membranes.

4.1. Coion exclusion

In principle, we desire coion exclusion for practical applications (e.g., electrodialysis), as it enhances ion exchange membrane selectivity, preferring the penetration of counterions over coions in (enthalpic) electric field-driven transport, while reducing salt (total ion) partitioning during entropic–driven transport [7,41–43]. Now, we address the earlier inquiry by investigating the influence of coion condensation on the partitioning performance of ion exchange membranes.

We have observed a decrease in the membrane's effectiveness in excluding coions as the external salt solution concentration increases. This trend is evident in Fig. 3, where we observe a rise in the (total) coion partition ratio when we increase the external solution concentration. Expressed mathematically within the framework of the ideal Donnan model, the (free) coion partition ratio can be formulated as a function involving the exponential of the electrical potential, Ψ, of the membrane. To this end, we know that the electrical potential, Ψ, intensity depends on a ratio between the density of the fixed charge group and the concentration of the external salt solution, namely $\rho_F/\overline{\rho}_{\text{salt}}$ [32]. Consequently, a heightened external solution concentration reduces the magnitude of the electrical potential, Ψ, across the interface, diminishing the capacity of the membrane to exclude external coions. In simpler terms, the coion partitioning increases with the higher concentration of the external salt solution, signaling the weakening of the ability of the membrane to reject the coions. For example, when increasing the concentration of the 2:1 salt solution from 10^{-3} to 1 mol/L, there is an approximately five–fold increase in the coion partitioning level.

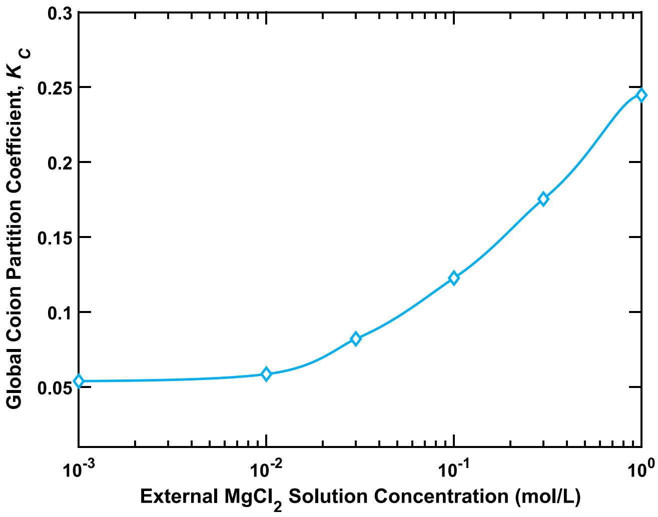

Fig. 3. Total (free and condensed) coion partition ratio between the cation exchange membrane and the 2:1 external salt solution. For the calculation here, we use sorbed concentration of coion per swollen polymer.

Fig. 4 distinguishes and quantifies the sorbed coion in its free (blue bars) and condensed (red bars) relaxation states, responding to the external 2:1 salt concentration changes. The overall sorbed coion concentration tends to reduce as the external salt concentration decreases, leading to a significant increase in the fraction of condensed coions compared to free ones. In particular, the condensed coion state dominates in the low-concentration external salt regime, i.e., at 0.001 mol/L. This observation enhances our understanding of why the ideal Donnan model fails to explain membranes' behavior within low-concentration salt solutions. The ideal model oversight of coion condensation as a driving force governing partitioning behavior becomes problematic at this low-concentration regime. However, as the concentration of the external salt solution increases, the condensed state vanishes. This phenomenon, on the other hand, explains the effectiveness of the Donnan model in capturing the coion exclusion property of membranes within the high-concentration salt regime, as the sorbed coions predominantly exist in the free state. According to Eq. (11), the condensed coion concentration, ρ_C^P, relies on the membrane's electrical potential, Ψ, the binding energy, U, and osmotic pressure, Π.

With an elevation in the external salt concentration, we observe a weakening of the electrical potential, Ψ, at the interface between the solution and the membrane, as seen in Fig. 2, reducing condensed coion concentration in the membranes, as visualized in Fig. 4.

The key takeaway from this discussion is that the phenomenon of coion condensation in charged membranes becomes crucial when the ratio of external salt concentration to fixed charge group density falls below a certain threshold. In our case, for example, when the ratio $\overline{\rho}_{\text{salt}}/\rho_F$ reaches $\approx 10^{-4}$, this phenomenon becomes significant. This concept gains particular importance in the context of developing membranes with high/ultra charge densities, as recently explored by Kamcev's group [44], exceeding charge densities of 3 mol/L in swollen membranes. In practical terms, when dealing with highly charged ion exchange membranes operating in multivalent salt solutions at commonly used concentrations, accurately assessing their selectivity performance requires careful consideration of the effects of coion condensation.

4.2. Counterion sorption

In our theoretical framework, the membranes undergo coion condensation facilitated by condensed divalent counterions, i.e., the 1:1 charged monomer-divalent counterion complex. To gain a more comprehensive understanding of the factors contributing to the low

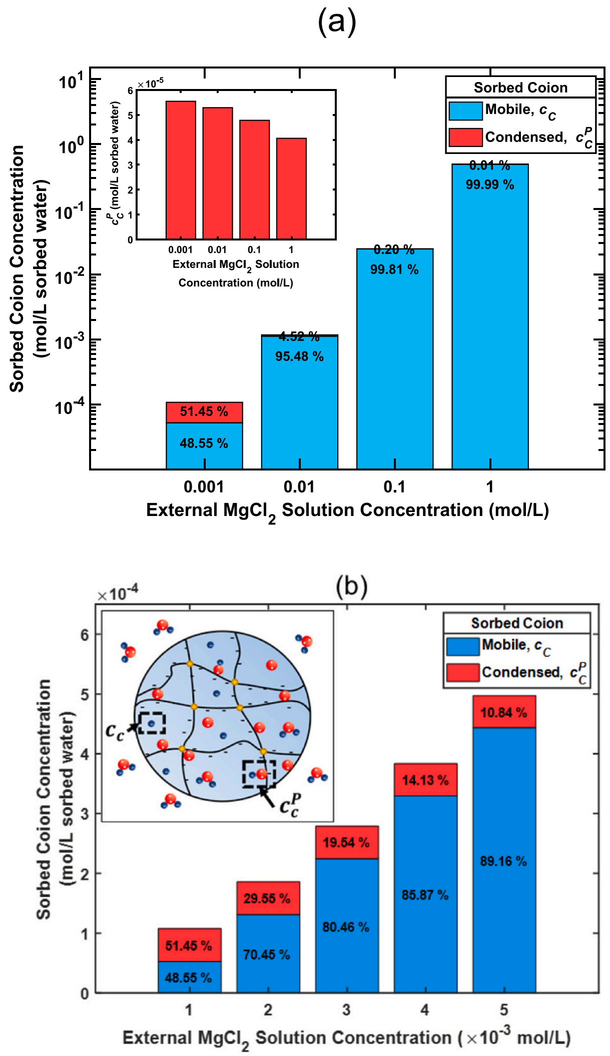

Fig. 4. (a) Free and condensed/paired coion concentrations as a function of the concentration of 2:1 external salt solution. (b) Enhanced visualization of sorbed concentration in the membranes exposed to external solution concentrations ranging from 1 to 5 × 10^{-3} mol/L. As a reminder to our reader, herein, we use the terms (i) "paired" and "site condensed" and (ii) "mobile" and "free" interchangeably. We note that the sum of the percentages in each bar equals 100 %.

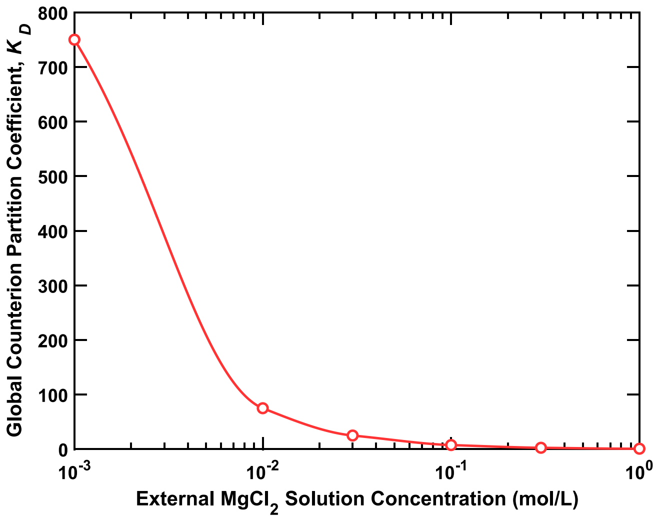

Fig. 5. Total (free and condensed) counterion partition ratio between the cation exchange membrane and the 2:1 external salt solution. For the calculation here, we use sorbed concentration of counterion per swollen polymer.

concentration of condensed coions within the membranes, we aim to quantify the occurrences of distinct divalent condensed counterion states: the 1:1 and 2:1 ones, alongside the population of free sorbed counterions within the membranes. This analysis effectively delineates the available binding/pairing sites where the sorbed coions could potentially condense. Due to the relatively low concentration of condensed coions along the polymer chains, we anticipate that the 1:1 interactions (one monomer to one divalent counterion complexation) will demonstrate less pronounced behavior than their 2:1 counterparts, where two charged monomers bind to a single divalent counterion complex.

We initiate our counterion investigation by analyzing Fig. 5, depicting the divalent counterion partition ratio between the membranes and external 2:1 salt solutions. This ratio quantifies the counterions' permeation capacity through polymeric membranes, i.e., the explicit interaction between the counterions and the charged membrane. Within a range consistent with prior research [13], we systematically varied the salt concentrations from 0.001 to 1 mol/L. As the salt concentration escalates, the partition ratio diminishes due to the attenuation of attractive forces, particularly the electrostatic sorption forces referred to as Donnan forces (see Fig. 2). The examined membranes are characterized by negatively charged fixed monomers on crosslinked polymeric chains, consistently resulting in a counterion partition ratio exceeding or, in some instances, close to 1. This outcome signifies a consistent positive partitioning trend. In other words, the overall net charge of the membranes remains unaltered across the tested salt concentration range, averting scenarios where (i) counterion concentration in the external solution significantly surpasses the sorbed concentration and (ii) a positive electrical potential (Ψ) emerges from a negative one. Our future investigations will delve into charge reversal phenomena linked to polymeric membranes submerged in multivalent salt solutions [45], addressing conditions (i) and (ii).

Until now, our counterion analysis has primarily focused on the global interaction between the membranes and the 2:1 external salt solutions, limiting our understanding of how the sorbed counterions interact within the polymer chains and the interstitial solution. To deepen our understanding of this microenvironment, we investigated local partitioning. Specifically, we examined the behavior of these sorbed counterions within the membranes. This exploration was crucial in identifying distinct counterion condensation complexes: a 1:1 interaction involving a divalent counterion and a charged monomer and a 2:1 complex involving a divalent counterion and two charged monomers. Notably, only the 1:1 counterion condensation type allows for subsequent condensation with a coion, due to the complex interplay of many-body electrostatic interactions. Our next step involves quantifying the different counterion states in the membranes. This quantification, as visualized in Fig. 6, differs from Fig. 5, which illustrates how sorbed counterions relax locally.

Fig. 6 presents the distribution of sorbed counterions in two distinct states: free and condensed. Our model consistently predicts that the total concentration of sorbed counterions remains stable across the varying salt concentrations, with a minor increase observed in the high-concentration salt solutions. Specifically, we see a slight rise of sorbed counterion concentration as the external solution concentration increases from 0.1 to 1.0 mol/L, in line with our previous research [13,25]. Moreover, the sorbed divalent counterion concentration is approximately half that of the fixed charge group density, thereby maintaining electroneutrality. In contrast to our prior work, this study introduces a novel perspective to our established theoretical framework. We can now explore two distinct relaxation states of condensed counterions within the membranes. Here, we allow sorbed counterions to bind physically to one or two charged monomers on the polymeric

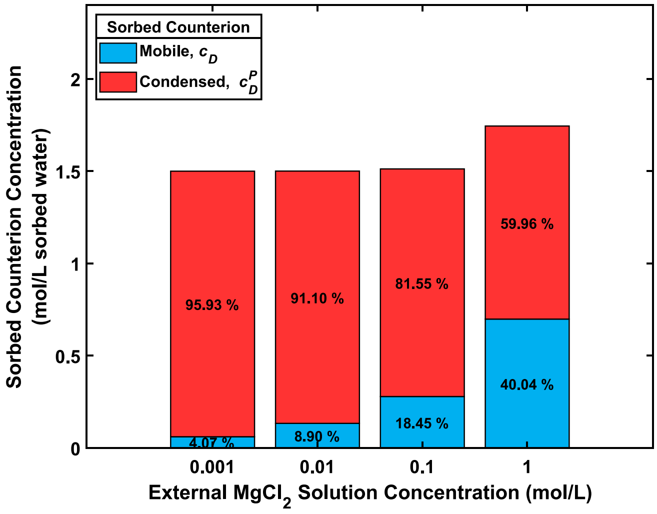

Fig. 6. Quantification of paired/condensed and mobile/free sorbed counterions in the membrane immersed in a 2:1 external salt solution.

chains. This approach enables us to consider the site-bound condensation of coions in the membranes. The findings presented in Fig. 6 underscore the prevalence of condensed counterions within the membranes. Notably, our results indicate a reduction in the fraction of condensed counterions; for instance, as the external solution concentration increases from 0.01 to 1.0 mol/L, the condensed counterion proportion decreases significantly from 91 % to 60 % within the membranes. This decrease permits a more substantial percentage of counterions to exist in the free state, subsequently enhancing the ionic conductivity of the membranes within this high-concentration salt range.

Fig. 7 demonstrates the prevailing presence of the 2:1 physically bound complex—bridged counterions—across various concentrations of the external salt solution. In essence, our findings indicate a higher occurrence of one counterion interacting with two charged monomers than one counterion binding to a single charged monomer. This conclusion is grounded in our assumption that each monomer carries a single, univalent charge, enabling the physical binding of a divalent counterion to either one or two monomers. We attain local electroneutrality within the 2:1 complexes. Our study primarily focuses on the interaction between a single-charged monomer and a divalent ion to capture the condensation of coions within the membranes. Notably, as the external salt concentration rises from 0.001 to 1.0 mol/L, there is a ten-fold reduction in the non-bridged condensed counterions (1:1 and 1:1:1 complexes) concentration. Consequently, elevated 2:1 external salt concentrations lead to fewer binding sites for coions—represented by the 1:1 complex— limiting coion condensation onto the polymeric chains. Conversely, at low salt concentrations (0.001 mol/L), coion binding sites increase, resulting in the dominance of the condensed coion species within the membranes, as depicted in Fig. 4. These observations shed light on the importance of condensed coions compared to their free state in the membranes, governing the exclusion and selectivity performance at low external multivalent solution concentrations.

5. Conclusions

Here, our study delves into the molecular factors governing the coion exclusion phenomenon within ion exchange membranes immersed in 2:1 salt solutions. By establishing a comprehensive theoretical framework encompassing coion and counterion condensation phenomena, we systematically examine the interplay between condensation, electrostatics, dielectric properties, and steric effects, elucidating their collective influence on the transport characteristics of ion exchange membranes. To validate our proposed theoretical framework, we apply it to dissect the experimental electrical potential measurements, denoted as Ψ, of a cation exchange membrane across varying concentrations of a 2:1 salt solution. We have compared our numerical results with the dataset reported by the research groups of Freeman and Crumlin and have found a significant agreement between them. Our investigations underscore a noteworthy trend: the waning impact of coion condensation as the concentration of the external salt solution escalates. In more

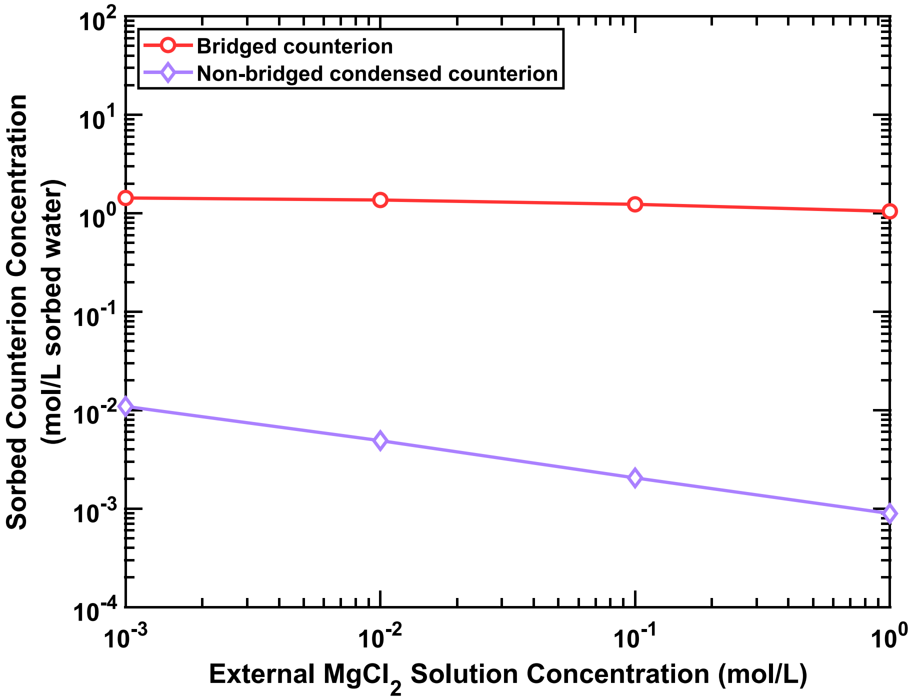

Fig. 7. Quantification of bridged (2:1, two charged monomers–one divalent counterion, interaction) and non–bridged (1:1, one charged monomer–one divalent counterion, and 1:1:1, one charged monomer–one divalent counterion-one monovalent coion, interactions) states in the cation exchange membrane.

accessible terms, heightened concentrations of the external salt lead to reduced available binding sites for sorbed coions to condense upon. This phenomenon can be attributed to the diminishing occurrence of the 1:1 complex formed between a charged monomer and a divalent counterion. As a consequence, the dominance shifts toward sorbed coions existing in an unbound/free state within high-concentration salt regimes. These discernments highlight the validity of the ideal Donnan model within environments characterized by elevated salt concentrations. Here, the coion condensation effect becomes progressively inconsequential, substantiating the applicability of Donnan model in such scenarios. Ultimately, our outcomes substantially enrich the comprehension of coion exclusion attributes exhibited by ion exchange membranes across a spectrum of salt solution concentrations, spanning from low to high.

CRediT authorship contribution statement

Zheng Jie Lim: Conceptualization, Methodology original and draft writing, Computation and analysis of results.

Marcus Kho: Conceptualization, Methodology original, Computation and analysis of results.

William Toh: Software and analysis of results.

Xiao Chen: Methodology and Supervision and Funding.

K.B. Goh: Conception and design of the work, Acquisition, Data analysis and editing of the draft and Funding.

Declaration of competing interest

The authors declare that they have no known competing financial interests or personal relationships that could have appeared to influence the work reported in this paper.

Data availability

Data will be made available on request.

Acknowledgments

K.B. Goh received support from the Ministry of Higher Education through the Fundamental Research Grant Scheme (FRGS/1/2023/STG07/MUSM/03/2), as well as the Monash University Malaysia Seed Grant (SED-000052). Xiao Chen's research was funded by the National Natural Science Foundation of China (No. 12202247), and the Postdoctoral International Exchange Program (funded by China Postdoc Council).

Appendix A. Supplementary data

Supplementary data to this article can be found online at https://doi.org/10.1016/j.desal.2023.117179.

References

[1] P. Zuo, Z. Xu, Q. Zhu, J. Ran, L. Ge, X. Ge, L. Wu, Z. Yang, T. Xu, Ion exchange membranes: constructing and tuning ion transport channels, Adv. Funct. Mater. (2022) 2207366.

[2] N. Ulbricht, A. Boldini, C. Bae, T. Wallmersperger, M. Porfiri, Solvation-driven actuation of anion-exchange membranes, Adv. Mater. Interfaces 9 (2022) 2200888.

[3] X. Li, Z. Qin, Y. Deng, Z. Wu, W. Hu, Development and challenges of biphasic membrane-less redox batteries, Adv. Sci. (2022) 2105468.

[4] J. Cheng, W. Zhou, M. Zhu, Z. Zhang, Y. Lu, Y. Chen, H. Mu, C. Lian, H. Liu, Optimizing microstructure of polyelectrolyte ion exchange membrane for electrodialysis, Chem. Eng. J. 468 (2023) 143669.

[5] B. Zhang, H. Tang, C. Liu, M. Wang, W. Li, Y. Shen, W. Shi, Microfiltration pretreatment of polymer-flooding produced wastewater before desalination: role of ca2+ and mg2+ in membrane fouling, Desalination 539 (2022) 115934.

[6] E.S. Jang, J. Kamcev, K. Kobayashi, N. Yan, R. Sujanani, S.J. Talley, B.D. Freeman, Effect of water content on sodium chloride sorption in cross-linked cation exchange membranes, Macromolecules 52 (6) (2019) 2569–2579.

[7] J. Kamcev, D.R. Paul, B.D. Freeman, Effect of fixed charge group concentration on equilibrium ion sorption in ion exchange membranes, J. Mater. Chem. A 5 (2017) 4638–4650.

[8] M. Galizia, F.M. Benedetti, D.R. Paul, B.D. Freeman, Monovalent and divalent ion sorption in a cation exchange membrane based on cross-linked poly (p-styrene sulfonate-co-divinylbenzene), J. Membr. Sci. 535 (2017) 132–142.

[9] R. Wang, R. Duddu, S. Lin, Extended donnan-manning theory for selective ion partition and transport in ion exchange membrane, J. Membr. Sci. 681 (2023) 121782.

[10] S. Mafé, P. Ramírez, J. Manzanares, Activity coefficients and coion exclusion in charged polymeric membranes with macroscopic inhomogeneities, Colloid Polym. Sci. 275 (1997) 599–603.

[11] S. Mafé, P. Ramírez, J. Pellicer, Activity coefficients and donnan coion exclusion in charged membranes with weak-acid fixed charge groups, J. Membr. Sci. 138 (1998) 269–277.

[12] M. Tedesco, H. Hamelers, P. Biesheuvel, Nernst-planck transport theory for (reverse) electrodialysis: I. Effect of co-ion transport through the membranes, J. Membr. Sci. 510 (2016) 370–381.

[13] X. Chen, K. Goh, Quantifying the coupled monovalent and divalent ions sorption in dense ion-exchange membranes, J. Membr. Sci. 666 (2023) 121140.

[14] G. Chen, K. Wei, A. Hassanvand, B. Freeman, S. Kentish, Single and binary ion sorption equilibria of monovalent and divalent ions in commercial ion exchange membranes, Water Res. 175 (2020) 115681.

[15] Y. Ji, H. Luo, G.M. Geise, Specific co-ion sorption and diffusion properties influence membrane permselectivity, J. Membr. Sci. 563 (2018) 492–504.

[16] L. Jones, P.N. Pintauro, H. Tang, Coion exclusion properties of polyphosphazene ion-exchange membranes, J. Membr. Sci. 162 (1999) 135–143.

[17] J. Kamcev, M. Galizia, F.M. Benedetti, E.-S. Jang, D.R. Paul, B.D. Freeman, G. S. Manning, Partitioning of mobile ions between ion exchange polymers and aqueous salt solutions: importance of counter-ion condensation, Phys. Chem. Chem. Phys. 18 (2016) 6021–6031.

[18] Z. Mai, S. Gui, J. Fu, C. Jiang, E. Ortega, Y. Zhao, W. Tu, W. Mickols, B. Van der Bruggen, Activity-derived model for water and salt transport in reverse osmosis membranes: a combination of film theory and electrolyte theory, Desalination 469 (2019) 114094.

[19] M. Tanaka, A.Y. Grosberg, Giant charge inversion of a macroion due to multivalent counterions and monovalent coions: molecular dynamics study, J. Chem. Phys. 115 (2001) 567–574.

[20] J. Hua, M.K. Mitra, M. Muthukumar, Theory of volume transition in polyelectrolyte gels with charge regularization, J. Chem. Phys. 136 (2012) 134901.

[21] M. Muthukumar, J. Hua, A. Kundagrami, Charge regularization in phase separating polyelectrolyte solutions, J. Chem. Phys. 132 (8) (2010).

[22] F. Horkay, I. Tasaki, P.J. Basser, Osmotic swelling of polyacrylate hydrogels in physiological salt solutions, Biomacromolecules 1 (2000) 84–90.

[23] A. Diehl, Y. Levin, Effective charge of colloidal particles, J. Chem. Phys. 121 (2004) 12100–12103.

[24] A. Kundagrami, M. Muthukumar, Theory of competitive counterion adsorption on flexible polyelectrolytes: divalent salts, J. Chem. Phys. 128 (2008) 244901.

[25] X. Chen, B. Rajendran, Q.-M. Liu, X.-Q. Feng, K.B. Goh, Divalent ion partitioning through dense ion exchange membranes, J. Membr. Sci. 687 (2023) 122077.

[26] M. Galizia, G.S. Manning, D.R. Paul, B.D. Freeman, Ion partitioning between brines and ion exchange polymers, Polymer 165 (2019) 91–100.

[27] J. Yu, N. Jackson, X. Xu, Y. Morgenstern, Y. Kaufman, M. Ruths, J. De Pablo, M. Tirrell, Multivalent counterions diminish the lubricity of polyelectrolyte brushes, Science 360 (2018) 1434–1438.

[28] J. Yu, N.E. Jackson, X. Xu, B.K. Brettmann, M. Ruths, J.J. De Pablo, M. Tirrell, Multivalent ions induce lateral structural inhomogeneities in polyelectrolyte brushes, Sci. Adv. 3 (2017) eaao1497.

[29] D. Kitto, J. Kamcev, Manning condensation in ion exchange membranes: a review on ion partitioning and diffusion models, J. Polym. Sci. 60 (2022) 2929–2973.

[30] A.M. Rumyantsev, A. Pan, S. Ghosh Roy, P. De, E.Y. Kramarenko, Polyelectrolyte gel swelling and conductivity vs counterion type, cross-linking density, and solvent polarity, Macromolecules 49 (2016) 6630–6643.

[31] S. Meng, R. Wang, X. Meng, Y. Wang, W. Fan, D. Liang, M. Zhang, Y. Liao, C. Tang, Reaction heterogeneity in the bridging effect of divalent cations on polysaccharide fouling, J. Membr. Sci. 641 (2022) 119933.

[32] B. Rajendran, I.K. Koo, X. Wang, X. Chen, K. Goh, How mechanical loading modulates non-ideal cosolute partitioning in hydrated polymeric membranes, J. Membr. Sci. 685 (2023) 121943.

[33] M. Li, B. Zhuang, J. Yu, Effects of ion valency on polyelectrolyte brushes: a unified theory, Macromolecules 55 (23) (2022) 10450–10456.

[34] K. Dill, S. Bromberg, Molecular driving forces: statistical thermodynamics in biology, chemistry, physics, and nanoscience, Garland Sci. (2010).

[35] R.J. Nap, M. Tagliazucchi, I. Szleifer, Born energy, acid-base equilibrium, structure and interactions of end-grafted weak polyelectrolyte layers, J. Chem. Phys. 140 (2014) 024910.

[36] K.B. Goh, H. Li, K.Y. Lam, Effects of salt-and oxygen-coupled stimuli on the reactive behaviors of hemoglobin-loaded polymeric membranes, Electrochim. Acta 297 (2019) 307–318.

[37] H. Zhang, G.M. Geise, Modeling the water permeability and water/salt selectivity tradeoff in polymer membranes, J. Membr. Sci. 520 (2016) 790–800.

[38] P. Aydogan Gokturk, R. Sujanani, J. Qian, Y. Wang, L.E. Katz, B.D. Freeman, E. J. Crumlin, The donnan potential revealed, Nat. Commun. 13 (2022) 5880.

[39] J. Kamcev, D.R. Paul, B.D. Freeman, Equilibrium ion partitioning between aqueous salt solutions and inhomogeneous ion exchange membranes, Desalination 446 (2018) 31–41.

[40] K. Goh, H. Li, K. Lam, Modeling the urea-actuated osmotic pressure response of urease-loaded hydrogel for osmotic urea biosensor, Sens. Actuators B 268 (2018) 465–474.

[41] L. Wang, T. Cao, K.E. Pataroque, M. Kaneda, P.M. Biesheuvel, M. Elimelech, Significance of co-ion partitioning in salt transport through polyamide reverse osmosis membranes, Environ. Sci. Technol. 57 (2023) 3930–3939.

[42] K. Goh, Z. Li, X. Chen, Q. Liu, T. Wu, Reaction-diffusion model to quantify and visualize mass transfer and deactivation within core-shell polymeric microreactors, J. Colloid Interface Sci. 608 (2022) 1999–2008.

[43] B. Dortdivanlioglu, N.E.D. Yilmaz, K. Goh, X. Zheng, C. Linder, Swelling-induced interface crease instabilities at hydrogel bilayers, J. Elast. (2021) 1–17.

[44] D. Kitto, J. Kamcev, The need for ion-exchange membranes with high charge densities, J. Membr. Sci. 677 (2023) 121608.

[45] S.C. Osorio, P. Biesheuvel, J. Dykstra, E. Virga, Nanofiltration of complex mixtures: the effect of the adsorption of divalent ions on membrane retention, Desalination 527 (2022) 115552.